A Role for Plant KASH Proteins in Regulating Stomatal Dynamics[1][OPEN]

Alecia Biel,[a] Morgan Moser,[a] and Iris Meier[a,b,2,3]

[a]Department of Molecular Genetics, The Ohio State University, Columbus, Ohio 43210
[b]Center for RNA Biology, The Ohio State University, Columbus, Ohio 43210

ORCID IDs: 0000-0001-5159-3385 (A.B.); 0000-0003-1471-607X (M.M.); 0000-0002-4141-5400 (I.M.).

Stomatal movement, which regulates gas exchange in plants, is controlled by a variety of environmental factors, including biotic and abiotic stresses. The stress hormone abscisic acid (ABA) initiates a signaling cascade, which leads to increased H_2O_2 and Ca^{2+} levels and F-actin reorganization, but the mechanism of, and connection between, these events is unclear. SINE1, an outer nuclear envelope component of a plant Linker of Nucleoskeleton and Cytoskeleton complex, associates with F-actin and is, along with its putative paralog SINE2, expressed in guard cells. Here, we have determined that Arabidopsis (*Arabidopsis thaliana*) SINE1 and SINE2 play an important role in stomatal opening and closing. Loss of SINE1 or SINE2 results in ABA hyposensitivity and impaired stomatal dynamics but does not affect stomatal closure induced by the bacterial elicitor flg22. The ABA-induced stomatal closure phenotype is, in part, attributed to impairments in Ca^{2+} and F-actin regulation. Together, the data suggest that SINE1 and SINE2 act downstream of ABA but upstream of Ca^{2+} and F-actin. While there is a large degree of functional overlap between the two proteins, there are also critical differences. Our study makes an unanticipated connection between stomatal regulation and nuclear envelope-associated proteins, and adds two new players to the increasingly complex system of guard cell regulation.

Eukaryotic nuclei are double membrane-bound organelles with distinct but continuous inner nuclear membranes (INM) and outer nuclear membranes (ONM). The site where the INM and ONM meet forms the nuclear pore, where nucleocytoplasmic transport occurs (Jevtić et al., 2014). Spanning the INM and the ONM are protein complexes known as linker of the nucleoskeleton and cytoskeleton (LINC) complexes. LINC complexes contribute to nuclear morphology, nuclear movement and positioning, chromatin organization and gene expression, and have been connected to human diseases (Chang et al., 2015; Lv et al., 2015). LINC complexes are composed of Klarsicht/ANC-1/Syne Homology (KASH) ONM proteins and Sad1/UNC-84 (SUN) INM proteins that interact in the lumen of the nuclear envelope (NE), thus forming a bridge between the nucleoplasm and the cytoplasm.

Opisthokonts (animals and fungi) and plants have homologous SUN proteins with C-terminal SUN domains located in the NE lumen. However, no proteins with sequence similarity to animal KASH proteins have been discovered in plants and thus much less is known regarding the function of plant LINC complexes (Graumann et al., 2010; Oda and Fukuda, 2011). Within the past few years, studies identifying structurally similar plant KASH protein analogs have stimulated increased interest in this area (Zhou et al., 2012, 2014, 2015; Graumann et al., 2014). Arabidopsis (*Arabidopsis thaliana*) ONM-localized WPP domain-interacting proteins (WIPs) were the first identified plant analogs of animal KASH proteins, binding the SUN domain of Arabidopsis SUN1 and SUN2 in the NE lumen (Zhou et al., 2012). WIP1, WIP2, and WIP3 form a complex with WPP-interacting tail-anchored protein1 (WIT1) and WIT2. Together, they are involved in anchoring the Ran GTPase activating protein (RanGAP) to the NE (Zhou et al., 2012), in nuclear movement in leaf mesophyll and epidermal cells and root hairs (Zhou et al., 2012; Tamura et al., 2013; Zhou and Meier, 2013; Tamura et al., 2015), and in nuclear movement in pollen tubes (Zhou and Meier, 2014; Zhou et al., 2015).

Based on similarity to the SUN-interacting C-terminal tail domain of WIP1 to WIP3, additional plant-unique KASH proteins were identified and named "SUN domain-interacting NE proteins" (SINE1 to SINE4 in Arabidopsis; Zhou et al., 2014). Arabidopsis SINE1 and SINE2 are putative paralogs and are conserved among

[1]This work was supported by a grant from the National Science Foundation (NSF-1613501 to I.M.).

[2]Author for contact: meier.56@osu.edu.

[3]Senior author.

The author responsible for distribution of materials integral to the findings presented in this article in accordance with the policy described in the Instructions for Authors (www.plantphysiol.org) is: Iris Meier (meier.56@osu.edu).

A.B. and I.M. conceived and planned the experiments; A.B. performed and analyzed most of the experiments; M.M. performed and analyzed the ROS experiment; A.B. and I.M. and wrote the article with assistance by M.M.; I.M. supervised the project and provided funding.

[OPEN]Articles can be viewed without a subscription.

www.plantphysiol.org/cgi/doi/10.1104/pp.19.01010

land plants (Poulet et al., 2017). In leaves, SINE1 is exclusively expressed in guard cells and the guard cell developmental lineage, whereas SINE2 is expressed in trichomes, epidermal and mesophyll cells, and only weakly in mature guard cells (Zhou et al., 2014). Both SINE1 and SINE2 are also expressed in seedling roots and share an N-terminal domain with homology to armadillo (ARM). Proteins encoding ARM repeats have been reported to bind actin and act as a protein–protein interaction domain in a multitude of proteins across both plant and animal kingdoms (Coates, 2003). SINE1 was verified to associate with F-actin via its ARM domain through colocalization studies in *Nicotiana benthamiana* leaves and Arabidopsis roots, but SINE2 does not share this property (Zhou et al., 2014). Furthermore, depolymerization of F-actin by latrunculin B (LatB) disrupts GFP-SINE1 localization in guard cells and increases GFP-SINE1 mobility during FRAP analysis, suggesting a SINE1-F-actin interaction in guard cells. Mutant analysis showed that SINE1 is required for the symmetric, paired localization of nuclei in guard cells, while SINE2 contributes to plant immunity against the oomycete pathogen *Hyaloperonospora Arabidopsis* (Zhou et al., 2014).

Stomatal dynamics rely on highly coordinated and controlled influx and efflux of water and ions that increase turgor pressure to facilitate opening and decrease turgor for stomatal closing. This process is mediated through complex signal transduction pathways, being controlled by plant and environmental parameters such as changes in light conditions and abiotic and biotic stresses (Schroeder et al., 2001b). Light changes result in a conditioned stomatal response in which stomata open and close in a daily cyclic fashion. Abiotic stresses such as drought, and biotic stresses such as pathogen exposure, can both override this daily cycle to induce a specific stomatal response.

The plant hormone abscisic acid (ABA) senses and responds to abiotic stresses, with ABA metabolic enzymes regulated by changes in drought, salinity, temperature, and light (Zhang et al., 2008a; Xi et al., 2010; Verma et al., 2016). ABA initiates long-term responses, such as growth regulation, through alterations in gene expression (Kang et al., 2002; Fujita et al., 2005) and induces stomatal closure as a short-term response to stress, involving the activation of guard cell anion channels and cytoskeleton reorganization (Eun and Lee, 1997; Zhao et al., 2011; Jiang et al., 2012; Li et al., 2014). F-actin is radially arrayed in open guard cells of several diverse plant species and undergoes reorganization into a linear or diffuse bundled array upon stomatal closure (Kim et al., 1995; Xiao et al., 2004; Li et al., 2014; Zhao et al., 2016). Although many disparate players have been shown to be important for regulating stomatal dynamics, it is still unclear how these events are interconnected and where actin reorganization fits in.

Here, we have investigated if Arabidopsis SINE1 and SINE2 play a physiological role in guard cell biology. Our findings show that both SINE1 and SINE2 are involved in stomatal opening and closing. Loss of SINE1 or SINE2 results in ABA hyposensitivity and impaired stomatal dynamics but does not affect pathogen-induced stomatal closure from the bacterial peptide flg22. The ABA-induced stomatal closure phenotype is, in part, attributed to impairments in Ca^{2+} and actin regulation.

RESULTS

SINE1 and SINE2 Are Involved in Light Regulation of Stomatal Opening and Closing

To assess whether SINE1 and SINE2 have a function in guard cell dynamics, we first monitored stomatal aperture changes in *sine1-1*, *sine2-1*, and *sine1-1 sine2-1* mutants under short-day conditions (8-h light, 16-h dark) using in vivo stomatal imprints from attached leaves. Two hours before light exposure, average stomatal apertures were between 2.8 and 3.3 μm (Fig. 1A). By midday, after 4 h of light exposure, wild-type stomata were fully opened, while *sine1-1* and *sine2-1* stomata had only opened marginally, and *sine1-1 sine 2-1* behaved more like wild type. Expression of proSINE1:GFP-SINE1 in *sine1-1* (SINE1:*sine1-1*) or proSINE2:GFP-SINE2 in *sine2-1* (SINE2:*sine2-1*) partially restored stomatal responsiveness to changes in light conditions. On average, neither *sine1-1* nor *sine2-1* stomata were fully open or fully closed for the duration of the assay.

To further assess stomatal opening, detached leaves from wild type and *sine* mutants (*sine1-1*, *sine2-1*, and *sine1-1 sine2-1*) were incubated in buffers containing Ca^{2+}, K^+, Ca^{2+} and K^+, or neither ion (Fig. 1B). Similar to methods described in Li et al. (2014) and Zhao et al. (2011), whole leaves were incubated in specified buffer throughout the duration of the assay and epidermal peels were taken and mounted just before imaging. In the absence of external K^+ and Ca^{2+} (opening buffer [OB] base), light-induced stomatal opening was impaired in *sine1-1*, *sine2-1*, and *sine1-1 sine2-1* (Fig. 1B, top left). With exposure to external Ca^{2+}, *sine1-1*, *sine2-1*, and *sine1-1 sine2-1* still displayed significantly impaired stomatal opening (Fig. 1B, top right). Likewise, with exposure to external K^+, statistically significant impairment during opening was observed in both single and double mutants (Fig. 1B, bottom left). After exposure to both Ca^{2+} and K^+, stomatal opening in *sine1-1* and *sine2-1* was still somewhat reduced compared to wild type (Fig. 1B, bottom right), but less so than when one or both ions were missing. Similar positive effects of low concentrations of Ca^{2+} on stomatal opening have been described in Hao et al. (2012) and Wang et al. (2014). In all assays, SINE1:*sine1-1* and SINE2:*sine2-1* displayed similar opening to wild type, indicating full rescue of the mutant phenotypes. Finally, dark-induced stomatal closure was assessed by comparing leaves transitioned from 3 h of light to 3 h of dark to those kept under constant light. *sine1-1*, *sine2-1*, and *sine1-1 sine2-1* were significantly impaired in this closing response, suggesting that SINE1 and SINE2 are also required for dark-induced stomatal closure (Fig. 1C).

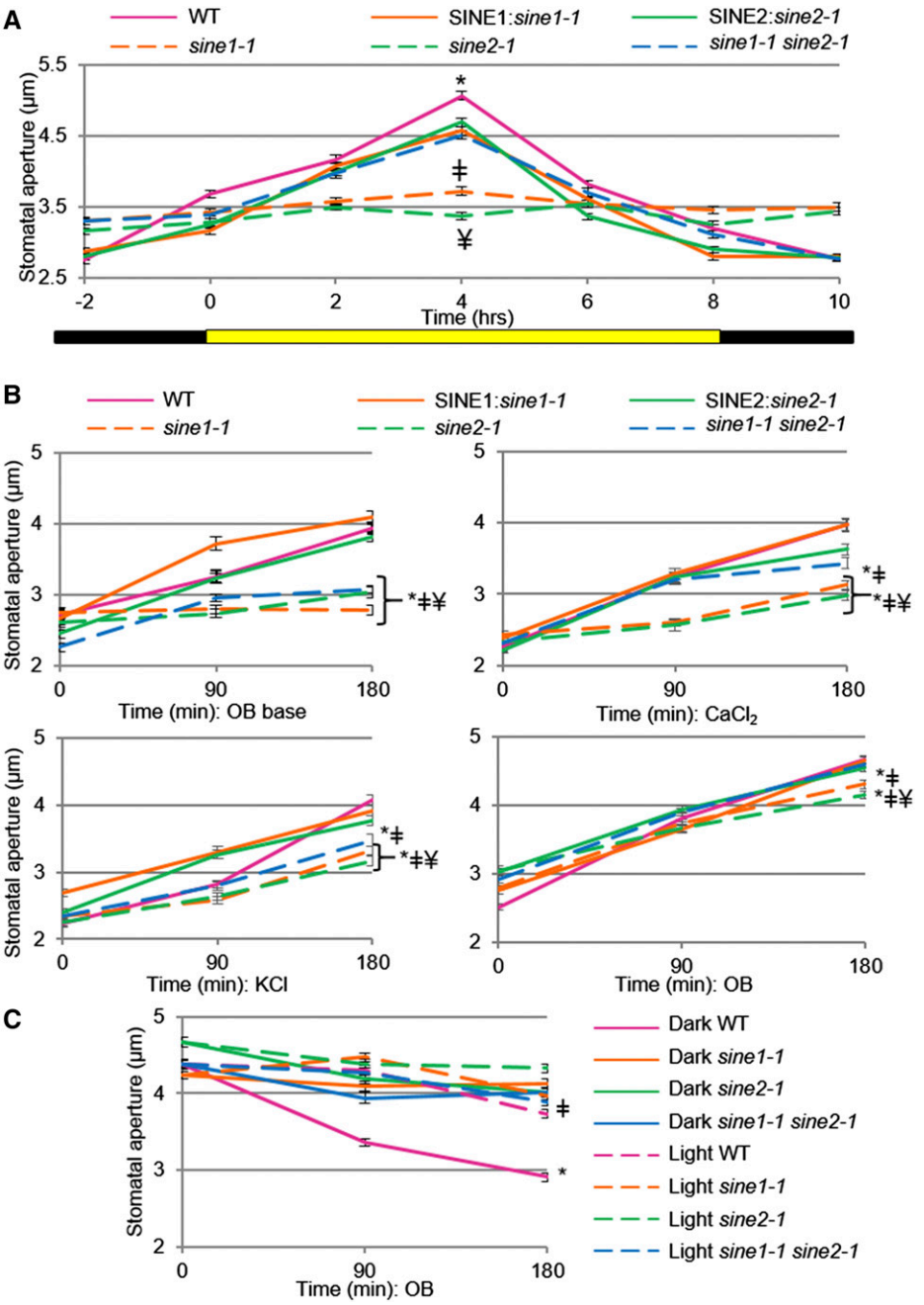

Figure 1. Determining the role of SINE1 and SINE2 in the light regulation of stomatal dynamics. A, Stomatal imprints from intact whole Arabidopsis leaves were taken and stomatal apertures were measured 2 h before the onset of lights (yellow bar) and every 2 h thereafter until 2 h after lights off (black bar). Symbols denote statistical significance as determined by Student's *t* test, with $P < 0.001$. *Wild type (WT) versus all other lines; ‡*sine1-1* versus wild type, SINE1:*sine1-1*, and *sine1-1 sine2-1*; ¥*sine 2-1* versus wild type, SINE2:*sine2-1*, and *sine1-1 sine2-1*. B, Whole leaves were placed in specified buffer for 3 h under constant light at the end of a night cycle, epidermal peels were mounted every 90 min, and stomatal apertures were measured. Top left, OB base (see "Materials and Methods"). Top right, OB base plus 10 μM of $CaCl_2$. Bottom left, OB base plus 20 mM of KCl. Bottom right, OB base plus 10 μM of $CaCl_2$ and 20 mM of KCl. Symbols denote statistical significance as determined by Student's *t* test, with $P < 0.001$. *Specified lines versus wild type; ‡specified lines versus SINE1:*sine1-1*; ¥specified lines versus SINE2:*sine2-1*. C, Whole leaves were placed in OB under constant light for 3 h and either kept under constant light or placed in dark for an additional 3 h. Epidermal peels were taken and stomatal apertures were measured every 90 min after the initial 3-h stomatal opening phase. Symbols denote statistical significance as determined by Student's *t* test, with $P < 0.001$. *Dark wild type versus light wild type; ‡dark *sine2-1* versus light *sine2-1*. A to C, All data are mean values ± SE from three independent experiments.

Together, these data indicate that SINE1 and SINE2 are involved in stomatal opening in response to white light and closing in response to dark, and that exogenous Ca^{2+} and K^+ can at least partially rescue opening.

Impaired ABA-Induced Stomatal Closure in *sine1-1* and *sine2-1*

ABA has been widely used to induce stomatal closure and monitor stomatal response to simulated abiotic stress (Umezawa et al., 2010) and was used here to test ABA stomatal response in *sine* mutants. Before this assay, we tested stomatal opening for all lines used here to ensure equal starting conditions for the closing assays (Supplemental Fig. S1).

Stomatal closure in response to ABA was observed as early as 1 h after exposure to 20 μM of ABA in all *sine* mutants when compared to wild type (Fig. 2A). Wild-type stomata continued to close over the following 2 h, while *sine1-1* (Fig. 2A, left), *sine2-1* (Fig. 2A, right), and *sine1-1 sine2-1* (Fig. 2A, left and right) did not exhibit further stomatal closure (representative images for wild type and *sine1-1* shown in Fig. 2B). In this assay, *sine1-1 sine2-1* stomatal closure resembled that of *sine1-1* and *sine2-1* single mutants. This suggests that there is no

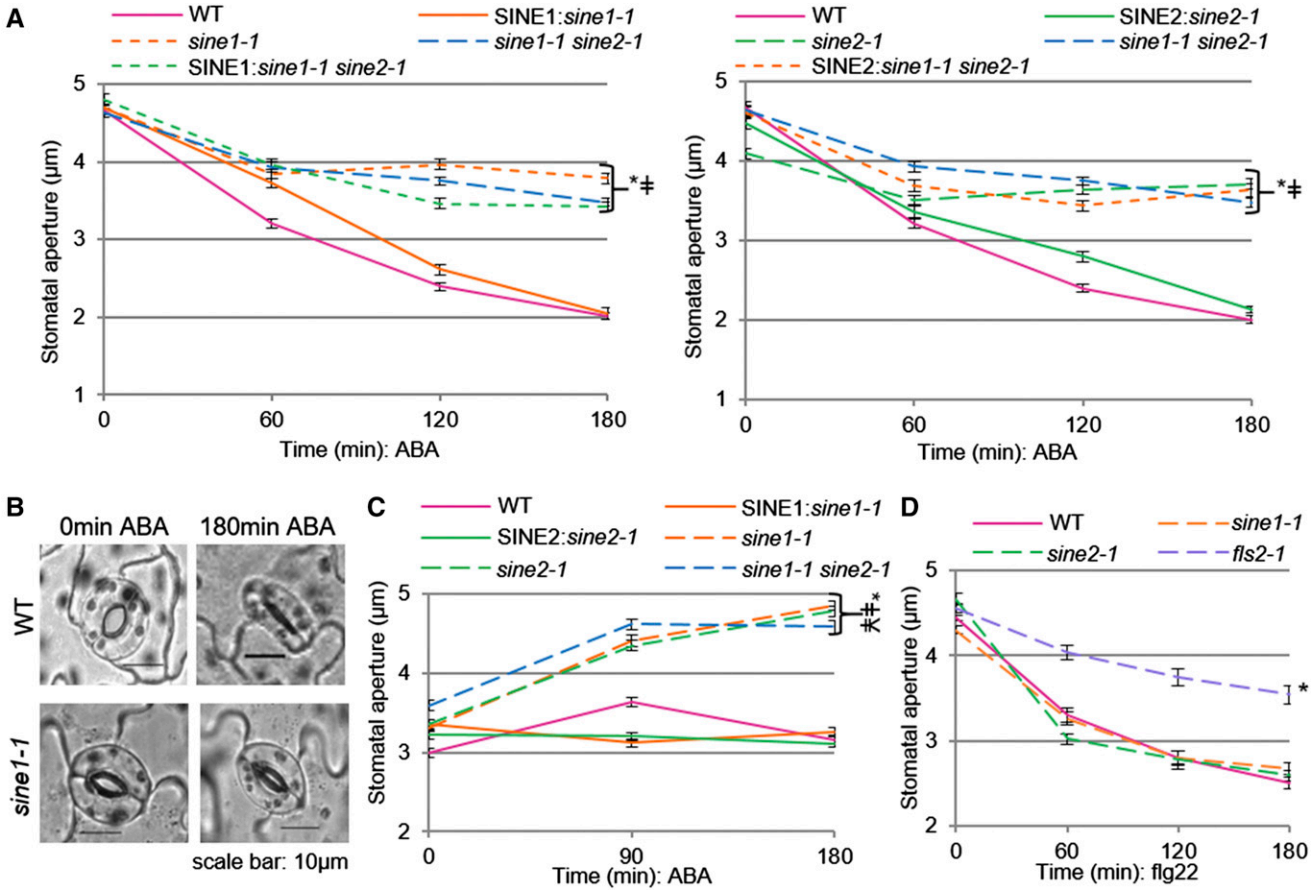

Figure 2. Abiotic versus biotic stress induced stomatal changes in *sine* mutants. Stomatal opening and closing assays were used here as described in "Materials and Methods." A, Leaves incubated in 20 μM of ABA during closure. All data were collected at the same time but are split here into two representations for clarity. Wild-type (WT) and *sine1-1 sine2-1* traces are therefore shown twice. B, Representative images of stomata for wild-type and *sine1-1* lines before and after ABA exposure. Scale bars = 10 μm. C, Leaves were incubated in OB plus 20 μM of ABA during stomatal opening. D, Leaves incubated in 5 μM of flg22 during closure. All data are mean values ± SE from three independent experiments. Symbols denote statistical significance as determined by Student's *t* test, with $P < 0.001$. *Specified lines versus wild type; ‡specified lines versus SINE1:*sine1-1*; ¥specified lines versus SINE2:*sine2-1*.

additive effect of the *sine1-1* and *sine2-1* mutants in this response, indicating SINE1 and SINE2 are working in the same pathway.

Exogenous ABA induced stomatal closure in SINE1:*sine1-1* and SINE2:*sine2-1* at a similar rate to wild type (Fig. 2A). To determine if both SINE1 and SINE2 are independently required in ABA-induced stomatal closure, the following partially complemented lines were used: SINE1pro:GFP-SINE1 in *sine1-1 sine2-1* (SINE1:*sine1-1 sine2-1*), and SINE2pro:GFP-SINE2 in *sine1-1 sine2-1* (SINE2:*sine1-1 sine2-1*; Zhou et al., 2014). Upon ABA exposure, SINE1:*sine1-1 sine2-1* and SINE2:*sine1-1 sine2-1* showed significantly impaired stomatal closure compared to wild type. Hence, neither SINE1 nor SINE2 alone is sufficient to rescue the *sine1-1 sine2-1* phenotype, confirming that both proteins are independently required for this process.

To confirm the mutant phenotypes for additional alleles, the transfer-DNA (T-DNA) insertion mutants *sine1-3* and *sine2-2* were used and compared to the SINE1:*sine1-3* and SINE2:*sine2-2* complemented lines and the partially complemented lines SINE1:*sine1-3 sine2-2* and SINE2:*sine1-3 sine2-2* (Zhou et al., 2014). Similar results were obtained for an ABA-induced stomatal closure assay, confirming independence of the phenotypes from insertion position and genetic background (Supplemental Fig. S2). Therefore, only the *sine1-1* and *sine2-1* alleles were used for the subsequent assays.

In addition to inducing stomatal closure, ABA also inhibits stomatal opening (Yin et al., 2013). To test the role of SINE1 and SINE2 in this process, stomatal opening assays utilizing OB were performed in the presence of 20 μM of ABA (Fig. 2C). Under these conditions, wild type, SINE1:*sine1-1*, and SINE2:*sine2-1* are unable to open stomata in the presence of ABA. However, *sine1-1*, *sine2-1*, and *sine1-1 sine2-1* stomata are unimpeded in their ability to open, indicating loss of

SINE1 or SINE2 results in hyposensitivity to ABA for both opening and closing.

Stomatal closure can also be induced by biotic stresses, such as pathogen exposure (Zhang et al., 2008a; Guzel Deger et al., 2015). The bacterial elicitor flg22 is a well-studied and accepted tool to simulate pathogen-induced stomatal closure, and was therefore tested here. As a control, we used the LRR receptor-like kinase mutant *fls2-1*, which is unable to recognize and bind flg22 (Dunning et al., 2007). After exposure to 5 μM of flg22, *fls2-1* had significantly inhibited stomatal closure compared to wild type, while flg22-induced stomatal closure in *sine1-1* and *sine2-1* was similar to that of wild type (Fig. 2D). Together, these data indicate that SINE1 and SINE2 are working within the ABA pathway to regulate ABA-induced stomatal closure and ABA-inhibition of stomatal opening and that these roles are distinct from the flg22-induced stomatal closure pathway.

Drought Susceptibility Is Increased in *sine1-1* and *sine2-1* Plants after Stomatal Opening

If stomata are unable to close in response to stress, an increase in transpiration is expected (Kang et al., 2002; Mustilli et al., 2002). To test this for *sine* mutants, leaves detached at midday were kept in a petri dish and weighed collectively for each genotype. Fresh weight loss was similar in *sine2-1*, *sine1-1 sine2-1*, SINE1:*sine1-1*, and SINE2:*sine2-1* compared to wild type (Fig. 3A). Although *sine1-1* did show a statistically significant increase in fresh weight loss compared to wild type ($P < 0.05$), there was no difference observed between *sine1-1* and SINE1:*sine1-1*. Thus, there appears to be no conclusive difference in fresh weight loss among wild type, *sine1-1*, and *sine2-1*. To test if this is due to the fact that *sine1-1* and *sine2-1* were impaired both in opening and closing, we repeated the water loss assay with leaves first incubated for 3 h in OB. As a control, detached leaves were exposed to OB base (without Ca^{2+} or K^+, Fig. 3B). In this case, similar results were obtained as in the air-only treatment. However, after pre-exposure to OB, *sine1-1* and *sine2-1* leaves lost weight at a significantly faster rate than wild type, while SINE1:*sine1-1* and SINE2:*sine2-1* lost weight at similar rates as wild type. Conversely, *sine1-1 sine2-1* showed an intermediate phenotype with no statistically significant difference to wild type (Fig. 3C, $P < 0.05$). Leaf morphology of *sine1-1* and *sine2-1* agreed with these observations in that pre-exposure to OB led to more rapid wilting, as seen by increased leaf curling and shrinking compared to wild type (Fig. 3D).

In a second experimental setting, individual leaves were placed abaxial side up throughout the assay and weighed separately to avoid a potential influence of overlapping leaves (Supplemental Fig. S3, A and B). Also, an additional T-DNA allele combination for the double mutant (*sine1-3 sine2-2*) was added to exclude potential influence of the genetic background. In addition, two lines expressing SINE1 and SINE2 under control of the 35S promoter in a wild-type background were added: 35S:GFP-SINE1 in wild type (SINE1:wild type) and 35S:GFP-SINE1 in wild type (SINE2:wild type). These data largely recapitulated those shown in Figure 3, suggesting that different incubation conditions did not influence the assay. Both double mutants lost water at an intermediate rate compared to wild type and the single mutants (Supplemental Fig. S3C), again consistent with the leaf morphology at the end of the assay (Supplemental Fig. S3B). Together, this suggests that the combination of an opening and closing defect masks any transpiration phenotype. Thus, induced stomatal opening reveals increased drought susceptibility in *sine1-1*, *sine2-1*, and partially in *sine1-1 sine2-1*.

Mapping the Position of SINE1 and SINE2 in the Stomatal ABA Signaling Pathway

Upon ABA perception, a signaling cascade results in the induction of both H_2O_2 and Ca^{2+} (Pei et al., 2000; Umezawa et al., 2010; Zhao et al., 2011). To narrow down the position of SINE1 and SINE2 in the ABA-induced stomatal closure pathway, we investigated H_2O_2-induced and Ca^{2+}-induced stomatal closure. Stomatal closure was measured as described above, in response to either 0.5 mM of H_2O_2 or 2 mM of $CaCl_2$ (Zhao et al., 2011). Upon exposure to H_2O_2, stomatal closure was impaired in *sine1-1*, *sine2-1*, and *sine1-1 sine2-1* compared to wild type (Fig. 4, A and B). SINE1:*sine1-1* and SINE2:*sine2-1* displayed H_2O_2-induced stomatal closure similar to wild type (Fig. 4, A and B). Significantly reduced stomatal closure was seen in SINE1:*sine1-1 sine2-1* and SINE2:*sine1-1 sine2-1*, again confirming the single- and double-mutant results (Fig. 4, A and B).

When exposed to $CaCl_2$, *sine1-1*, and *sine2-1* were somewhat impaired in stomatal closure, which was also observed in the double mutant (Fig. 4, C and D). However, 2 mM of $CaCl_2$ more effectively triggered stomatal closure in *sine1-1*, *sine2-1*, and *sine1-1 sine2-1* than the previous treatments of ABA or H_2O_2 (Supplemental Table S1). Meanwhile, SINE1:*sine1-1* and SINE2:*sine2-1* lines showed stomatal closure similar to wild type in response to exogenous application of Ca^{2+} and SINE1:*sine1-1 sine2-1* and SINE2:*sine1-1 sine2-1* had a similar degree of stomatal closure as single and double *sine* mutants (Fig. 4, C and D). These results indicate that external Ca^{2+} is able to partially rescue the stomatal closure phenotype.

Within the ABA pathway, there is feedback between the Ca^{2+} and H_2O_2 branches (Pei et al., 2000; Desikan et al., 2004; Zou et al., 2015). Thus, we also tested the stomatal response of *sine1-1* and *sine2-1* to a combination of both inducers. With exposure to both Ca^{2+} and H_2O_2, stomatal closure was similar among *sine1-1 sine2-1*, *sine1-1 sine2-1*, wild type, SINE1:*sine1-1*, and SINE2:*sine2-1* (Fig. 4E). Finally, stomatal closure based on ABA, H_2O_2, Ca^{2+}, and darkness was expressed as

percentage of the aperture size at the beginning of the assay (Supplemental Table S2; see "Materials and Methods"). This did not lead to any change in the data interpretation described above. Together, these data show that the impaired stomatal closure response of SINE1 and SINE2 mutants can be partially rescued by external Ca^{2+}, but not by H_2O_2.

Stomatal Overexpression of SINE2 Leads to Compromised Stomatal Dynamics

SINE1 and SINE2 expression patterns differ with regards to guard cells and epidermal cells. Thus, we assessed the impact of their ubiquitous expression on stomatal dynamics. 35S:GFP-SINE1 in wild type (SINE1:WT) and 35S:GFP-SINE2 in wild type (SINE2:WT), respectively, were compared to SINE1pro:GFP-SINE1 (SINE1:*sine1-1*) and SINE2pro:GFP-SINE2 (SINE2:*sine2-1*). Confocal microscopy showed that SINE1:wild type and SINE1:*sine1-1* have similar expression levels in guard cells (Fig. 5, A, and B). However, as expected, SINE2:WT showed significantly higher GFP expression in guard cells than SINE2:*sine2-1*. Indeed, under the assay conditions, no GFP signal above background was detected in SINE2:*sine2-1*–expressing guard cells (Fig. 5, A and B). In contrast, immunoblots of protein extracts from whole seedlings and rosette leaves of SINE1:wild type, SINE2:WT, SINE1:*sine1-1*, and SINE2:*sine2-1* showed similar amounts of GFP fusion protein (Supplemental Fig. S4). This confirms that GFP-SINE2 is expressed in SINE2:*sine2-1* and indicates that SINE2:wild type leads to overexpression of GFP-SINE2 in guard cells compared to the native SINE2 promoter.

Next, we tested stomatal impairment in the SINE1 and SINE2 ubiquitously expressing lines. While SINE1:WT

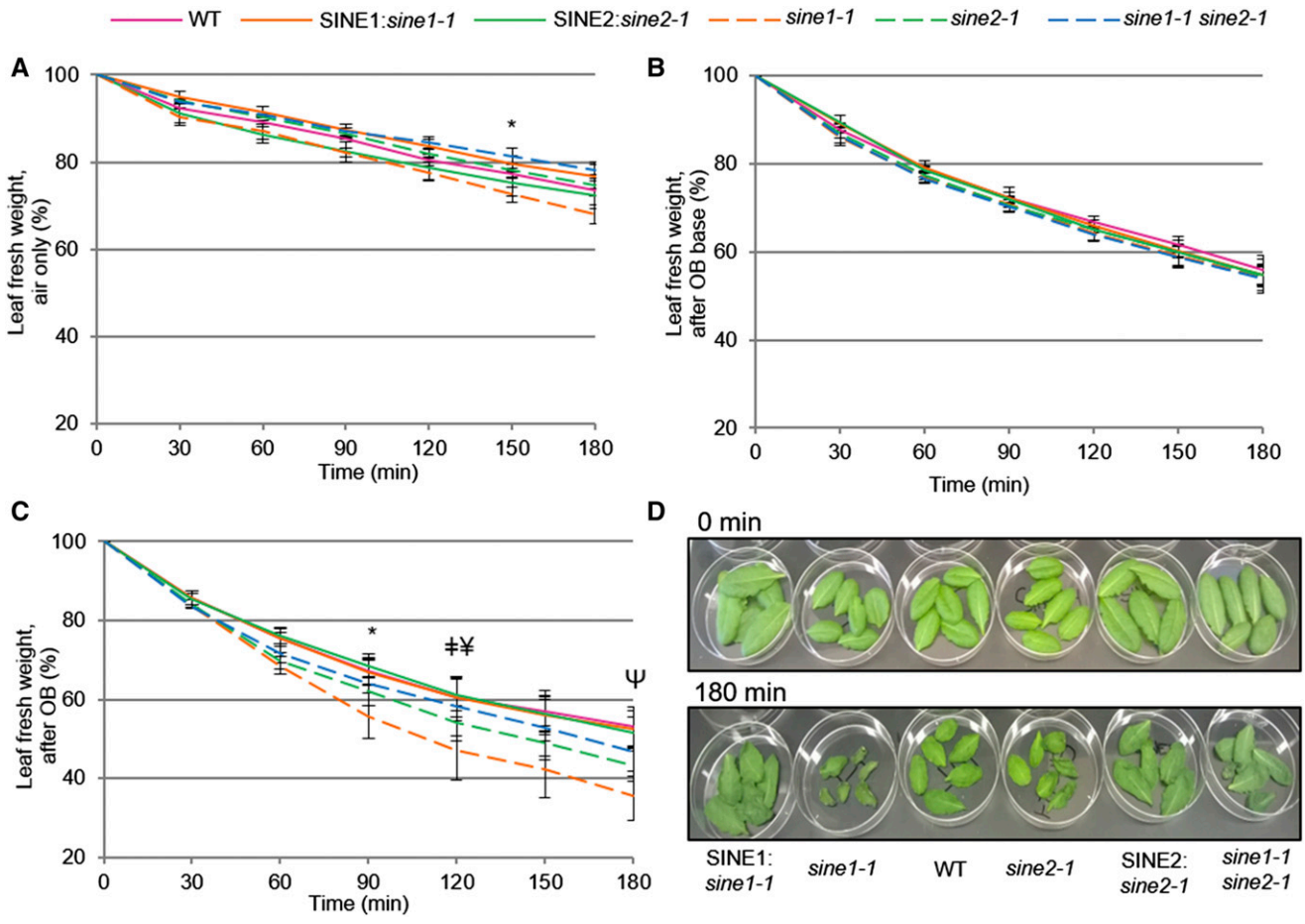

Figure 3. Transpiration rates after induced stomatal opening. Rosette leaves were taken from 6- to 8-week–old short-day plants at similar developmental stages for each of the lines depicted and kept abaxial side up. Fresh leaves were placed in specified buffer for 3 h under constant light, transferred to a petri dish as specified below, and weighed every 30 min thereafter. In air (A); in OB base (B); in OB (C) with representative images shown in (D) where the top images are leaves at 0 min before OB incubation and bottom images are leaves after 180 min OB incubation. Mean values ± SE from at least three independent experiments are shown in (A) to (C). B, No statistically significant differences. Symbols in (A) and (C) denote the beginning of statistically significant differences as determined by Student's *t* test, with $P < 0.05$. **sine1-1* versus wild type (WT); ‡*sine2-1* versus wild type; ¥*sine2-1* versus SINE2:*sine2-1*; d: *sine1-1* versus SINE1:*sine1-1*.

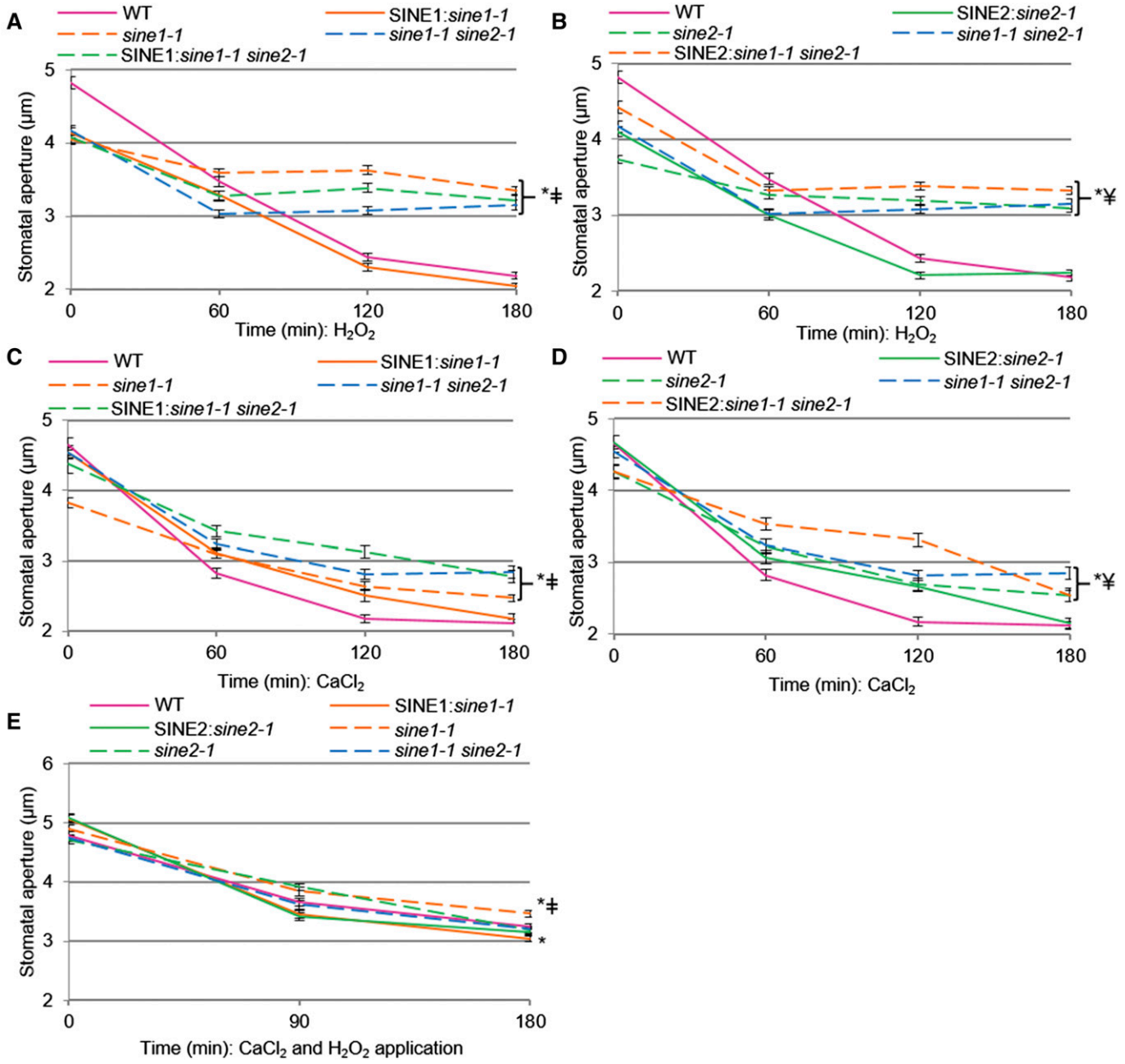

Figure 4. Stomatal closure in response to H_2O_2 and $CaCl_2$ for SINE1 and SINE2 mutants. Stomatal opening and closing assays were used here as described in "Materials and Methods." A and B, Leaves incubated in 0.5 mM of H_2O_2 during closure. Data obtained from one experiment and split into two representations for clarity. C and D, Leaves incubated in 2 mM of $CaCl_2$ during closure. Data obtained from one experiment and split into two representations for clarity. E, Leaves incubated in 0.5 mM of H_2O_2 plus 2 mM of $CaCl_2$ during closure. All data are mean values ± SE from three independent experiments. Symbols denote statistical significance as determined by Student's *t* test, with $P < 0.001$. *Specified lines versus wild type (WT); ‡specified lines versus GFP-SINE1:*sine1-1*; ¥specified lines versus GFP-SINE2:*sine2-1*.

behaved like wild type, SINE2:WT recapitulated the *sine1-1* phenotype during a light/dark cycle (Fig. 5C). Similarly, SINE2:WT was largely unresponsive to ABA, while SINE1:WT showed wild type-like stomatal closure (Fig. 5D). Thus, 35S promoter-driven GFP-SINE1 expression has no significant effect on SINE1/SINE2 function in guard cells. However, additional expression of the normally lowly expressed SINE2 in guard cells appears toxic to SINE1/SINE2 function. This suggests that fine-tuning of cellular abundance of the two proteins is required for their function. Because one model to account for the interference of SINE2 is that accumulation of a SINE1/SINE2 heterodimer could negatively affect a specific role of SINE1 in guard cells, we tested if the two proteins can interact in a split-ubiquitin yeast two-hybrid assay. Indeed, interaction was seen between

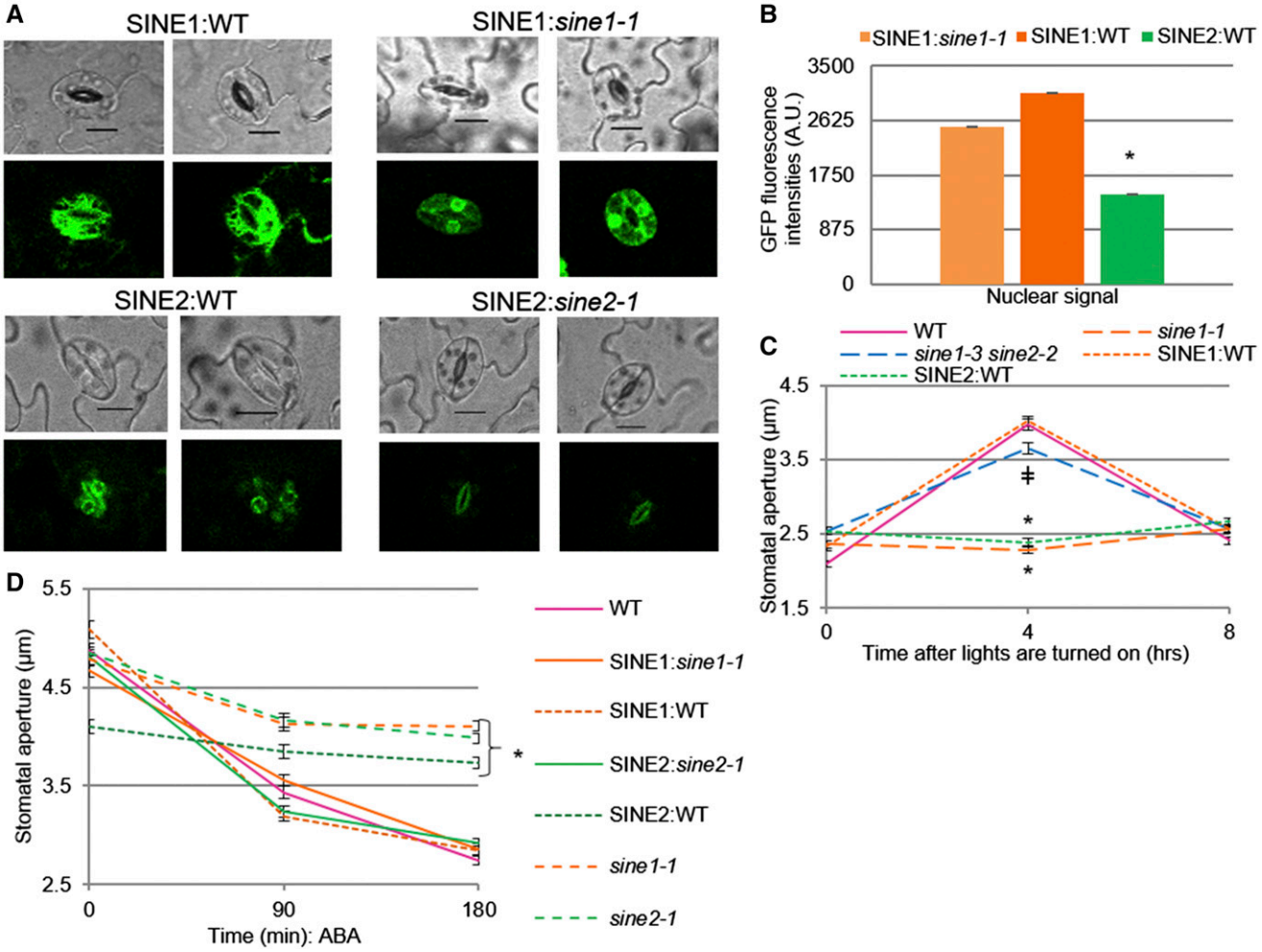

Figure 5. SINE2 but not SINE1 overexpression leads to compromised stomatal dynamics. A, Confocal microscopy was used to take images of plants expressing GFP-tagged SINE1 or SINE2, with representative images shown. Gain was set to first image of top row and used for the remaining images. Scale bars = 10 μm. B, Data taken from two plants. A quantity of ≥50 nuclei were measured for each line. Nuclear fluorescence intensities were measured using the software ImageJ (National Institutes of Health). SINE2:*sine2-1* had no measurable fluorescence signal at the nucleus and was therefore not quantified. Symbols denote statistical significance as determined by Student's *t* test. $^{*}P < 0.005$, SINE2:WT versus SINE1:*sine1-1*. C, Stomatal apertures taken from stomatal imprint assay at the start and end of light cycles. Symbols denote statistical significance as determined by Student's *t* test. $^{*}P < 0.001$, specified lines versus wild type (WT); $^{\ddagger}P = 0.004$, specified lines versus wild type. D, ABA induced stomatal closure assay as described in "Materials and Methods." Symbols denote statistical significance as determined by Student's *t* test, with $^{*}P <$ 0.001, specified lines versus wild type, SINE1:sine1-1, SINE1:WT, and SINE2:sine2-1. Data shown in (C) and (D) are from three independent experiments. Data are mean values ± SE.

SINE1 and SINE2 as well as a weak interaction between SINE2 and SINE2. Because of self-activation issues, the SINE1–SINE1 interaction could not be tested (Supplemental Fig. S5).

Although SINE2:WT recapitulates the *sine1-1* and *sine2-1* phenotype in both a light/dark cycle and in ABA response, this line showed wild-type–like loss of fresh weight during desiccation (Supplemental Fig. S3). This could be explained if SINE2:WT had a compensatory phenotype, such as altered stomatal density (SD). SINE2 is normally expressed only in mature guard cells, whereas SINE1 is expressed in both progenitor guard cells and mature guard cells (Zhou et al., 2014). We therefore tested if 35S promoter-driven SINE2 is also influencing stomatal development (Nadeau and Sack, 2002; Lucas et al., 2006). Indeed, both stomatal index (SI) and SD are reduced in SINE2:WT, but not in SINE1:WT, wild type, or the T-DNA insertion mutants, suggesting that a compensatory phenotype might indeed exist (Supplemental Fig. S6).

Together, these data show that ubiquitous expression of SINE2 impairs stomatal response to changes in light conditions as well as during ABA-induced stomatal closure. Additionally, ubiquitous SINE2 expression resulted in altered stomatal development. These data suggest that the abundance of SINE2 in guard cells

might be tightly controlled and linked to SINE1/2 function.

Interactions between *sine1-1* and *sine2-1* Mutants and the Actin Cytoskeleton

F-actin rearrangement has been implicated in stomatal dynamics and undergoes a specific pattern of reorganization (Staiger et al., 2009). When this actin rearrangement is disrupted, there are concomitant perturbations in stomatal dynamics (Kim et al., 1995; Xiao et al., 2004; Jiang et al., 2012; Li et al., 2014; Zhao et al., 2016). We tested here if the characterized *sine* mutants showed interactions with drug-induced F-actin depolymerization or with F-actin stabilization during stomatal closing. LatB results in F-actin depolymerization and facilitates stomatal closure in the presence of ABA (MacRobbie and Kurup, 2007). In contrast, jasplakinolide (JK) stabilizes and polymerizes F-actin, inhibiting stomatal closure (MacRobbie and Kurup, 2007; Li et al., 2014). We used LatB and JK in the presence and absence of ABA to assess their influence on stomatal closure in *sine1-1* and *sine2-1*.

When wild-type leaves are incubated in either OB or OB + LatB in the light, stomatal apertures remained open during the 3-h assay (Fig. 6A). Similarly, both OB and OB + LatB treatment of *sine1-1* and *sine2-1* resulted in open stomata throughout the assay (Fig. 6A). ABA alone and ABA + LatB induced stomatal closure in wild type, as reported in MacRobbie and Kurup (2007; Fig. 6A). ABA exposure in *sine1-1* and *sine2-1* resulted in minimal closure, as shown above. However, treatment with ABA and LatB resulted in significant closure of stomata in both *sine1-1* (Fig. 6A, left, $P < 0.001$) and *sine2-1* (Fig. 6A, right, $P < 0.001$), closely resembling wild type. This suggests that LatB treatment overcomes the inhibition of stomatal closure caused by the loss of either SINE1 or SINE2.

Both under OB and OB + JK, stomata remained open in wild type (Fig. 6B). JK inhibited ABA-induced closure in wild type, as previously reported, indicating that actin depolymerization is necessary for ABA-induced stomatal closure (MacRobbie and Kurup, 2007; Li et al., 2014). OB alone resulted in sustained stomatal opening in *sine1-1* mutants. JK treatment in the absence of ABA led to stomatal closure in *sine1-1* mutants, as did the combination of JK and ABA (Fig. 6B, left). In contrast, JK did not induce stomatal closure in *sine2-1* and did not rescue the *sine2-1* defect in ABA-induced stomatal closure (Fig. 6A, right). To account for any differences seen in starting aperture size, the percent of stomatal closure

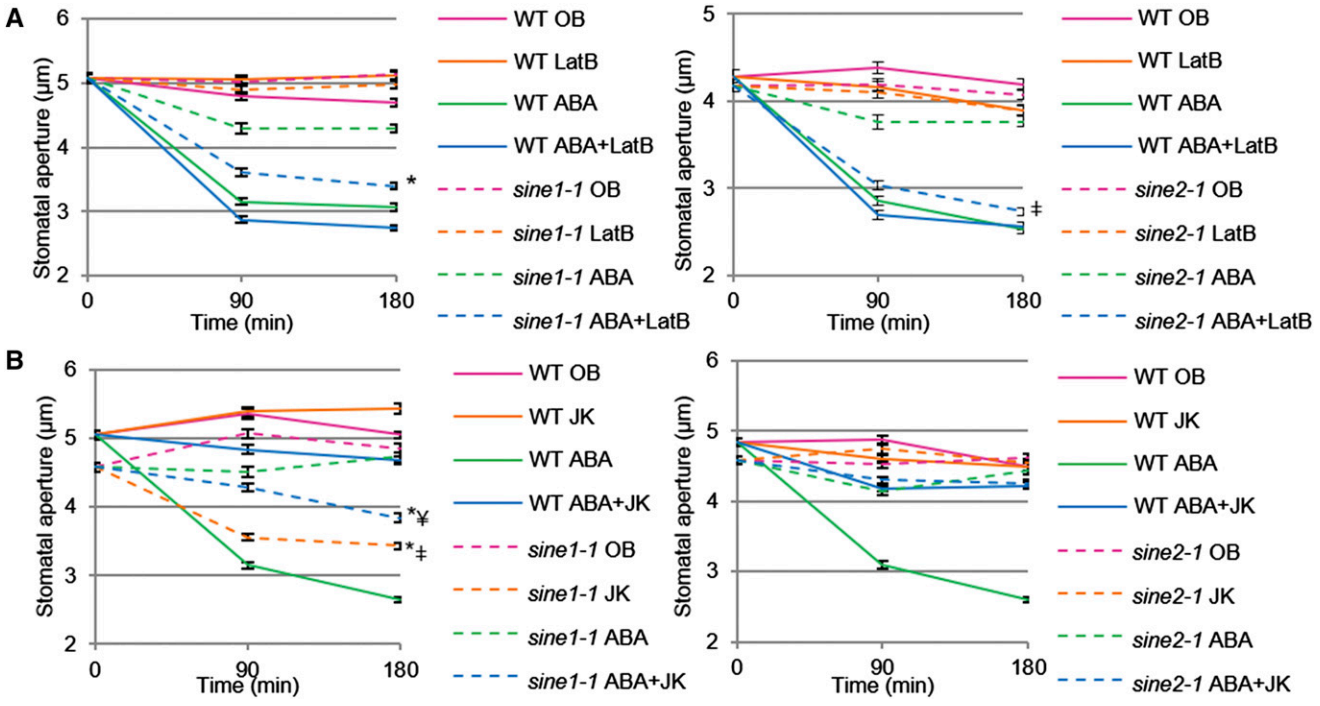

Figure 6. Disrupting actin dynamics in *sine1-1* and *sine2-1* mutant lines alters stomatal closure. Stomatal closure was monitored over a 3-h incubation time in the presence and absence of ABA and actin-disrupting drugs. A, Buffers with and without 20 μM of ABA and 10 μM of the F-actin depolymerizing drug LatB. Left, Wild type (WT) and *sine1-1*. Right, Wild type and *sine2-1*. Symbols denote statistical significance as determined by Student's *t* test, with $P < 0.001$. *sine1-1*, ABA+LatB versus *sine1-1*, ABA only; ‡*sine2-1*, ABA+LatB versus *sine2-1*, ABA only. B, buffers with and without 20 μM ABA and 10 μM of the F-actin–stabilizing drug JK. Left, Wild type and *sine1-1*. Right, Wild type and *sine2-1*. Symbols denote statistical significance as determined by Student's *t* test, with $P < 0.001$. *Specified lines versus *sine1-1*, ABA only; ‡*sine1-1*, JK only versus wild type, JK only; ¥*sine1-1*, ABA+JK versus wild type, ABA+JK. All data are mean values ± SE from three independent experiments.

was calculated (Supplemental Table S3) and the results are similar to those described above.

Together, these data indicate that actin depolymerization rescues the defect in ABA-induced stomatal closure that is caused by the loss of SINE1 or SINE2, and that in the absence of SINE1, JK-induced actin stabilization and polymerization can mimic the effect of ABA.

DISCUSSION

We have shown here that two related plant KASH proteins, SINE1 and SINE2, play similar, yet distinguishable, roles in stomatal dynamics in response to light, dark, and ABA. We have previously reported that in leaves, SINE1 is expressed in guard cells and the guard cell developmental lineage, while SINE2 is expressed predominantly in leaf epidermal and mesophyll cells, and only weakly detected in mature guard cells (Zhou et al., 2014). GFP fusion proteins of SINE1 and SINE2 decorate the NE, as expected based on their KASH-protein function, but SINE1 is also localized in a filamentous pattern that resembles actin in guard cells and mature root cells, and this localization can be abolished by actin-depolymerizing drugs (Zhou et al., 2014). In *sine1* mutant lines it was observed that the guard cell nuclei, which are typically arranged opposite each other in the center of the paired guard cells, are shifted from this position. This cellular phenotype was recapitulated in LatB-treated wild-type guard cells, suggesting actin involvement, but no effect was found in *sine2* mutants. Based on these cell biological data, we hypothesized a function for SINE1, but not necessarily for SINE2, in guard cell biology.

Interestingly, in most bioassays applied here, *sine1* and *sine2* mutants showed similar guard cell-related phenotypes, which were also recapitulated by the double mutant, suggesting that the two proteins act in a shared pathway required for wild-type–like guard cell function. Loss of either SINE1 or SINE2 greatly diminishes stomatal opening in response to light, as well as stomatal closing in response to dark or ABA and significantly reduces the dynamic range of stomatal apertures between night and midday (Figs. 1 and 2). The lack of responsiveness to light for stomatal opening could be compensated in both single and double mutants through addition of external potassium and a low concentration of Ca^{2+}. Both ions have been shown to play roles during light-induced stomatal opening (Hao et al., 2012; Wang et al., 2014), thus suggesting that the mutants might be hyposensitive to the external application of these ions (Fig. 1B).

During stomatal closure, ABA acts through Ca^{2+}-dependent and Ca^{2+}-independent signaling events (Wang et al., 2013). ABA increases both the Ca^{2+} entry at the plasma membrane and the internal Ca^{2+} release resulting in Ca^{2+} oscillations (Gilroy et al., 1991; Allen et al., 1999; Grabov and Blatt, 1999; Hamilton et al., 2000; Schroeder et al., 2001a; Jiang et al., 2014; An et al., 2016). The increase in cellular Ca^{2+} is connected to reactive oxygen species (ROS; Kwak et al., 2003; Ogasawara et al., 2008) and ultimately results in the activation of K^+ outward channels and slow and fast ion channels (SLAC/ALMT), as well as the inactivation of K^+ inward channels such as KAT1 (Jezek and Blatt, 2017). We therefore tested if application of the ROS H_2O_2 and/or Ca^{2+} could rescue the *sine* mutant stomatal closure phenotype. While H_2O_2 alone had no or a minimal effect, Ca^{2+} partially rescued the impaired stomatal closure phenotype and the combination of Ca^{2+} and ROS rescued the *sine* mutants to wild-type levels of closure (Fig. 4). Consistent with this finding, internal ROS increased after ABA exposure in *sine1-1* and *sine2-1* (Supplemental Fig. S7, A and B). In contrast, Fura-2 staining suggests that early cytoplasmic Ca^{2+} fluctuations after exposure to ABA are dampened in *sine1-1* and *sine2-1*, although it is important to note that all Fura-2 data must take into account possible signal degradation due to any uncleared AM ester (Supplemental Fig. S7, C–E; Kanchiswamy et al., 2014). Together, this suggests that, within ABA signaling, SINE1 and SINE2 act upstream of Ca^{2+}, and that ROS exposure might intensify the Ca^{2+}-based rescue, potentially through the described effect of ROS on activating the Ca^{2+} channels (Kwak et al., 2003; Wang et al., 2013; Jezek and Blatt, 2017).

Mutants with defects in stomatal regulation often show drought susceptibility phenotypes, due to their inability to fully close stomata and thus lose an excess of water through evaporation (Kang et al., 2002; Zhao et al., 2016). However, when detached *sine* single- and double-mutant rosette leaves were exposed to room air and monitored for fresh weight loss, no difference from wild-type leaves was observed (Fig. 3A). In light of the results of the light/dark assay (Fig. 1A) as well as the impairment in both light-induced opening and ABA- or dark-induced closing of stomata (Figs. 1, B and C, and 2A), we reasoned that mutant plants and detached mutant leaves might be less subject to evaporation because, on average, stomata neither fully open nor fully close. This was substantiated by testing evaporation sensitivity after fully opening stomata by incubation in OB. Under these conditions, mutant leaves wilted more rapidly, consistent with the observed defects in stomatal closure (Fig. 3).

When two lines that constitutively express SINE1 or SINE2 under control of the 35S promoter were added to this assay (Supplemental Fig. S3), both lines showed a fresh weight loss indistinguishable from wild-type plants. This is not surprising in the case of SINE1, given that this line showed no stomatal defects. Constitutive expression of SINE2, however, led to defects both in the light/dark assay and during ABA-induced stomatal closure (Fig. 5, C and D) that would be consistent with a *sine* mutant-like hypersensitivity to evaporation. To assess whether constitutive expression of SINE2 leads to additional—possibly compensatory—phenotypes, we calculated SD and SI of fully developed rosette leaves (Supplemental Fig. S6). Indeed, constitutive SINE2 expression leads to a reduction of both SD and SI. No such reduction was observed in any other line tested

(Supplemental Fig. S6). The reduced number of stomata caused by constitutive SINE2 expression might thus compensate for the closing defects in this line, and result in wild-type–like evaporation within the level of resolution of our assay. Notably, this additional phenotype suggests that the SINE gene family not only acts in stomatal function but might also play a role during stomatal development. Only SINE1 is expressed throughout the guard cell developmental lineage, and mis-expression of SINE2 might thus highlight a yet unexplored role for SINE1 in the guard cell developmental program.

It was noted that the *sine1-1 sine2-1* stomata respond differently from the *sine1-1* and *sine2-1* single mutants in the light/dark assay (Fig. 1A), but not in any of the subsequent assays. One notable difference between the light/dark assay and all other assays is that the former was performed on potted plants, using leaf imprints, while all other assays used detached leaves during treatments and epidermal peels for imaging. We thus argued that a whole plant phenotype might exist specifically in the double mutant that compensates for any stomatal dynamic defects seen in the light/dark assay. As SINE1 and SINE2 are highly expressed in the seedling root (Zhou et al., 2014), we investigated primary root and lateral root (LR) characteristics (Supplemental Fig. S8). Of the four parameters tested, three showed significant differences in only the *sine1-1 sine2-1* double mutant: decreased primary root length, number of LR, and LR density. No differences were observed in LR length. While it is currently unknown if this root morphology phenotype accounts for the behavior of the *sine1-1 sine2-1* mutant in the light/dark assay, these data demonstrate that the possibility of additional phenotypes unique to the double mutant have to be taken into account when interpreting these data.

Considerably less is known about the signal transduction pathway that triggers stomatal closure after exposure to dark. It is generally assumed, however, that many steps are shared with the ABA pathway (Jezek and Blatt, 2017). For example, mutants in the PYR/PYL/RCAR ABA receptors are also deficient in their stomatal response to darkness (Merilo et al., 2013). Similarly, diurnal rhythmicity is closely linked to the increase of guard cell ABA during the night—based both on de novo synthesis and import from the apoplast—and depletion of ABA levels during the day (Daszkowska-Golec and Szarejko, 2013). Together, these known connections are consistent with the *sine* mutant phenotypes observed here, and suggest a primary role for SINE1 and SINE2 in a step downstream of ABA, but upstream of Ca^{2+}.

There is a plethora of known effects of actin dynamics on stomatal aperture regulation (Kim et al., 1995; Eun et al., 2001; Lemichez et al., 2001; MacRobbie and Kurup, 2007; Gao et al., 2008, 2009; Hikagi et al., 2010; Zhao et al., 2011; Jiang et al., 2012; Li et al., 2014). Together with SINE1 association with F-actin in guard cells, this made us speculate whether the *sine* mutant phenotypes are related to disturbances in guard cell actin dynamics. It has been shown previously that the inhibitor of F-actin assembly LatB and the F-actin stabilizer JK have opposite effects on ABA-based stomatal closure (MacRobbie and Kurup, 2007). While LatB mildly enhanced closure in the presence of ABA, JK inhibited it. Our data recapitulate in Arabidopsis these effects reported for *Commelina communis* (MacRobbie and Kurup, 2007). Both *sine1* and *sine2* mutant phenotypes showed a clear interaction with the actin drugs. While loss of either SINE1 or SINE2 inhibited ABA-induced closure, coincubation with LatB rescued this inhibition to a significant degree (Fig. 6A). A hypothesis consistent with this finding is that SINE1 and SINE2 are connected to actin turnover during the transition from radial to longitudinal arrays that accompanies stomatal closure. In the presence of LatB, this activity would not be required. JK inhibited guard cell closure in both wild type and the *sine2-1* mutant, consistent with the assumption that actin de-polymerization is a required step. Surprisingly, JK alone, in the absence of ABA, was able to trigger stomatal closure in the *sine1-1* mutant (Fig. 6B). SINE1 might be required for an additional step involved in stabilizing F-actin, downstream of ABA, and this step might be also required for closing. In wild-type guard cells, this could be accomplished through ABA-triggered involvement of SINE1, and JK has therefore no further effect. However, this step could be inhibited in the absence of SINE1, and could thus be rescued by JK alone, mimicking the ABA response. More studies will be required to verify these proposed actin-related functionalities of the two proteins, but the data already show (1) that there is indeed an interaction between SINE1/2 function and actin worthy of further investigation, and (2) that while SINE1 and SINE2 have many overlapping functions, there are also critical differences, as revealed by the JK data. Future studies will have to focus on the real-time analysis of actin dynamics in the different mutant backgrounds and under the different treatments and the investigation of genetic interactions between *sine* mutants and the reported mutants of actin-modulating proteins involved in guard cell regulation.

In addition, it is possible that SINE1 and SINE2 influence vacuolar dynamics and/or vesical trafficking. It has been shown that >90% of solutes released from guard cells originate from vacuoles. F-actin binds to vacuolar ion channels, where it, together with cytoplasmic Ca^{2+}, regulates vacuolar K^+ release during ABA-induced stomatal closure (MacRobbie and Kurup, 2007; Kim et al., 2010). Furthermore, several studies have noted the involvement of actin in vesicle trafficking, in particular the transport and activation of the K^+ channel KAT1 in response to ABA (Leyman et al., 1999; Sutter et al., 2006, 2007; Sokolovski et al., 2008; Eisenach et al., 2012).

Together, we have shown that the two plant KASH proteins SINE1 and SINE2 function in stomatal aperture regulation in a variety of scenarios that involve light, dark, and ABA. We propose that they act downstream of ABA, and upstream of Ca^{2+} and actin. While there is a large degree of functional overlap between the

two proteins, there are also critical differences, and their further analysis might shed light on the role of their intriguingly different expression patterns. This study reveals an unanticipated connection between stomatal regulation and a class of NE proteins known to be involved in nuclear anchoring and positioning, and adds two new players to the ever more complex world of guard cell biology (Albert et al., 2017). Addressing the connection between the phenotypes described here and the cellular role of SINE1 in guard cell nuclear positioning will likely be one of the more groundbreaking avenues of further study.

MATERIALS AND METHODS

Plant Material

Arabidopsis (*Arabidopsis thaliana*; ecotype Col-0) was grown at 25°C in soil under 8-h light and 16-h dark conditions. For all assays, leaves were collected from 6- to 8-week–old Arabidopsis plants grown under these conditions. The *fls2-1* mutant has been reported in Uddin et al. (2017). *sine1-1* (SALK_018239C), *sine2-1* (CS801355), and *sine2-2* (CS1006876) were obtained from the Arabidopsis Biological Resource Center while *sine1-3* (GK-485E08-019738) was obtained from GABI-Kat (www.gabi-kat.de). All SINE1 and SINE2 lines used here were reported in Zhou et al. (2014).

Stomatal Aperture Measurements

Stomatal bioassays were performed by detaching the youngest, fully expanded rosette leaves of 6- to 8-week–old plants grown under short-day conditions (8-h light; 16-h dark).

For the light/dark assay, Duro Super Glue (item no. 1400336; Duro) was applied to a glass slide and the abaxial side of a leaf was pressed into the glue to create an imprint. Imprints were taken 2 h before the chamber lights turning on and every 2 h until 2 h after the lights were turned off. The imprints were allowed to dry and subsequently imaged to obtain stomatal aperture measurements.

All other stomatal assays involved placing leaves in a petri dish abaxial side up with OB containing 10 mM of MES, 20 μM of $CaCl_2$, 50 mM of KCl, and 1% (w/v) Suc at pH 6.15 for 3 h under constant light, while leaves remained whole until designated time points at which abaxial epidermal strips were carefully peeled and imaged using a confocal microscope (Zhao et al., 2011; Li et al., 2014; Eclipse C90i, Nikon). While immediately peeling and mounting may lead to small variations in starting aperture size between experiments, stomata prepared in this way display opening and closing comparable to published fluctuations (Zhao et al., 2011; Li et al., 2014). For some of the experiments, OB base containing 10 mM of MES and 1% (w/v) Suc at pH 6.15 was used to test stomatal dynamics with and without addition of 20 μM of $CaCl_2$ and/or 50 mM of KCl. Stomatal closing assays were performed immediately after the opening assays, in which leaves were transferred to closing buffer containing 10 mM of MES at pH 6.15 with or without the following treatments, as indicated: 20 μM of ABA, 2 mM of $CaCl_2$, 0.5 mM of H_2O_2, or 5 μM of flg22 (Kang et al., 2002; Zhang et al., 2008b; Zhao et al., 2011). Leaves were placed in darkness to induce stomatal closure for 3 h when mentioned. The software NIS-Elements (Nikon Instruments) was used for stomatal aperture measurements.

Transpiration Assay

To monitor water loss, five to six fully expanded leaves were detached from each plant at similar developmental stages (sixth to ninth true rosette leaves). For the "air only" assay, leaves were placed adaxial side up in an open petri dish under constant light on a laboratory bench and leaf weights were recorded every 30 min (Kang et al., 2002). For all other assays in Figure 2, leaves were placed adaxial side up in either OB, OB base, OB base with 20 μM of $CaCl_2$, or OB base with 50 mM of KCl for 3 h to induce opening. Leaves were then dried briefly on Kimwipes (item no. 34120; Kimberly-Clark) and placed adaxial side up in dry petri dishes for an additional 3 h under constant light. Leaf weights were recorded every 30 min. For the transpiration assay in Supplemental Figure S2, leaves were placed abaxial side up in OB and then kept abaxial side up throughout the duration of the assay on paper towels. Leaves were weighed individually.

Confocal Microscopy and Fluorescence Intensity Measurements

For the imaging and quantification shown in Figure 5, A and B, 6- to 8-week–old Arabidopsis leaves were imaged using a confocal microscope (Eclipse C90i; Nikon). Image settings were established first for the highest expressing line (35S:GFP-SINE1 in wild type) to obtain a clearly visible, but not overexposed, GFP fluorescence signal at the NE. These settings were then applied for imaging all other samples: a medium pinhole with a gain setting of 7.35- and the 488-nm laser set at 15% power. All images were taken at room temperature with a Plan Fluor 40× oil objective (numerical aperture of 1.3; Nikon). The software NIS-Elements was used to quantify fluorescence by drawing a region of interest around individual guard cell nuclei.

ROS and Calcium Production Assays

Detection of ROS in stomata was performed as described in Li et al. (2014). Whole leaves were incubated in OB adaxial side up for 3 h under constant light. Leaves with open stomata were incubated in MES buffer pH 6.15 containing 50 μM of H_2DCF-DA in the dark for 15 min and then washed with water. The leaves were then transferred to closing buffer containing 20 μM of ABA for 15, 30, 60, or 120 min. At the indicated time points, abaxial epidermal strips were peeled from the leaves for ROS detection by confocal microscopy with a setting of 488-nm excitation and 525-nm emission. The experiments were repeated four times with at least 70 stomata for each time point.

Detection of Ca^{2+} in stomata was performed using the Fura-2 AM dye (CAS 108964-32-5; Sigma Aldrich; Jiang et al., 2014). Epidermal peels were floated in 10 mM of MES-TRIS (pH 6.1) buffer containing 1 μM of Fura-2 AM and kept at 4°C in the dark for 2 h. The Fura-2 dye was then washed out and peels were placed back in OB for 1 h at room temperature. ABA was added and time-lapse imaging of stomata was performed using confocal microscopy at specified time intervals. Z-stacks of stomata were taken at each time point and mean intensity projections were used for quantification. The software NIS-Elements was used to isolate and quantify cytoplasmic fluorescence to exclude chloroplast signals.

Immunoblotting

Nicotiana benthamiana leaves were collected and ground in liquid nitrogen into powder, and protein extractions were performed at 4°C. One milliliter of radioimmunoprecipitation buffer was used to extract 500 μL of plant tissue, as described in Zhou et al. (2014). After three washes in radioimmunoprecipitation buffer, samples were separated using 10% SDS-PAGE, transferred to polyvinylidene difluoride membranes (Bio-Rad Laboratories), and detected with a mouse anti-GFP (1:2,000; 632569; Takara Bio) or a mouse antitubulin (1:2,000; 078K4842; Sigma-Aldrich) antibody. Membranes were imaged using an Odyssey Clx Imaging system (LI-COR) and fluorescence was quantified using the software Image Studio (LI-COR).

Yeast Strains and Manipulations

All work with yeast was done using *Saccharomyces cerevisiae* strain NMY51:MATahis3D200 trp1-901 leu2-3,112 ade2 LYS2::(lexAop)4-HIS3 ura3::(lexAop)8-lacZ ade2::(lexAop)8-ADE2 GAL4 obtained from the DUAL Membrane Starter Kit N (Dualsystems Biotech; P01201–P01229). Yeast cells were grown using standard microbial techniques and media (Lentze and Auerbach, 2008). Media designations are as follows: yeast extract plus Ade medium, peptone, and Glc; and synthetic defined dropout (SD-dropout) medium. Minimal dropout media are designated by the constituent that is omitted (e.g. "−leu −trp −his −ade" medium lacks Leu, Trp, His, and Ade). Recombinant plasmid DNA constructs were introduced into NMY51 by LiOAc-mediated transformation as described in Gietz and Schiestl (2007).

Statistical Analyses

The number of stomata analyzed for each line, in all figures, is ≥80, unless otherwise stated. Error bars represent the SD of means. Asterisks or symbols denote statistical significance after Student's *t* test as indicated.

Accession Numbers

Sequence data from this article can be found in the GenBank/EMBL data libraries under accession numbers NM_148591 (SINE1) and NM_111268 (SINE2).

Supplemental Data

The following materials are available.

Supplemental Figure S1. Stomatal opening in *sine* mutants before exogenous application of ABA.

Supplemental Figure S2. Stomatal closure in response to ABA for *sine1-3* and *sine2-2* mutants.

Supplemental Figure S3. Transpiration rates of individual leaves after induced stomatal opening.

Supplemental Figure S4. Protein-blot analysis of transgenic Arabidopsis plants expressing GFP-SINE1 and GFP-SINE2.

Supplemental Figure S5. Interactions between SINE1 and SINE2 proteins in the membrane yeast two-hybrid system.

Supplemental Figure S6. SD and SI of fully developed rosette leaves.

Supplemental Figure S7. ROS production and cytoplasmic calcium monitoring in *sine* mutants.

Supplemental Figure S8. Root morphology of *sine* mutants.

Supplemental Table S1. Comparison of stomatal closure assays.

Supplemental Table S2. Percent stomatal closure for ABA and light-dark assays.

Supplemental Table S3. Percent stomatal closure for cytoskeleton drug treatment assays.

ACKNOWLEDGMENTS

We are grateful to Dr. Sarah Assmann (Penn State University) for critical reading of the first version of this article. We thank Andrew Kirkpatrick and all members of the Meier lab for fruitful discussions and Dr. Norman Groves of the Meier lab for proofreading, critiquing, and editing the final version of the article. We thank Dr. Xiao Zhou (Caribou Biosciences) for constructing the 35S-driven SINE1 and SINE2 expressing Arabidopsis lines while working in the Meier lab and Dr. David Mackey (Ohio State University) for the *fls2-1* mutant.

Received August 19, 2019; accepted November 10, 2019; published November 25, 2019.

LITERATURE CITED

Albert R, Acharya BR, Jeon BW, Zañudo JGT, Zhu M, Osman K, Assmann SM (2017) A new discrete dynamic model of ABA-induced stomatal closure predicts key feedback loops. PLoS Biol **15:** e2003451

Allen GJ, Kuchitsu K, Chu SP, Murata Y, Schroeder JI (1999) Arabidopsis abi1-1 and abi2-1 phosphatase mutations reduce abscisic acid-induced cytoplasmic calcium rises in guard cells. Plant Cell **11:** 1785–1798

An Y, Liu L, Chen L, Wang L (2016) ALA inhibits ABA-induced stomatal closure via reducing H_2O_2 and Ca^{2+} levels in guard cells. Front Plant Sci **7:** 482

Chang W, Worman HJ, Gundersen GG (2015) Accessorizing and anchoring the LINC complex for multifunctionality. J Cell Biol **208:** 11–22

Coates JC (2003) Armadillo repeat proteins: Beyond the animal kingdom. Trends Cell Biol **13:** 463–471

Daszkowska-Golec A, Szarejko I (2013) Open or close the gate—stomata action under the control of phytohormones in drought stress conditions. Front Plant Sci **4:** 138

Desikan R, Cheung MK, Bright J, Henson D, Hancock JT, Neill SJ (2004) ABA, hydrogen peroxide and nitric oxide signalling in stomatal guard cells. J Exp Bot **55:** 205–212

Dunning FM, Sun W, Jansen KL, Helft L, Bent AF (2007) Identification and mutational analysis of Arabidopsis FLS2 leucine-rich repeat domain residues that contribute to flagellin perception. Plant Cell **19:** 3297–3313

Eisenach C, Chen ZH, Grefen C, Blatt MR (2012) The trafficking protein SYP121 of Arabidopsis connects programmed stomatal closure and K^+ channel activity with vegetative growth. Plant J **69:** 241–251

Eun SO, Lee Y (1997) Actin filaments of guard cells are reorganized in response to light and abscisic acid. Plant Physiol **115:** 1491–1498

Eun SO, Bae SH, Lee Y (2001) Cortical actin filaments in guard cells respond differently to abscisic acid in wild-type and *abi1-1* mutant *Arabidopsis*. Planta **212:** 466–469

Fujita Y, Fujita M, Satoh R, Maruyama K, Parvez MM, Seki M, Hiratsu K, Ohme-Takagi M, Shinozaki K, Yamaguchi-Shinozaki K (2005) AREB1 is a transcription activator of novel ABRE-dependent ABA signaling that enhances drought stress tolerance in Arabidopsis. Plant Cell **17:** 3470–3488

Gao XQ, Chen J, Wei PC, Ren F, Chen J, Wang XC (2008) Array and distribution of actin filaments in guard cells contribute to the determination of stomatal aperture. Plant Cell Rep **27:** 1655–1665

Gao XQ, Wang XL, Ren F, Chen J, Wang XC (2009) Dynamics of vacuoles and actin filaments in guard cells and their roles in stomatal movement. Plant Cell Environ **32:** 1108–1116

Gietz RD, Schiestl RH (2007) High-efficiency yeast transformation using the LiAc/SS carrier DNA/PEG method. Nat Protoc **2:** 31–34

Gilroy S, Fricker MD, Read ND, Trewavas AJ (1991) Role of calcium in signal transduction of commelina guard cells. Plant Cell **3:** 333–344

Grabov A, Blatt MR (1999) A steep dependence of inward-rectifying potassium channels on cytosolic free calcium concentration increase evoked by hyperpolarization in guard cells. Plant Physiol **119:** 277–288

Graumann K, Runions J, Evans DE (2010) Characterization of SUN-domain proteins at the higher plant nuclear envelope. Plant J **61:** 134–144

Graumann K, Vanrobays E, Tutois S, Probst AV, Evans DE, Tatout C (2014) Characterization of two distinct subfamilies of SUN-domain proteins in Arabidopsis and their interactions with the novel KASH-domain protein AtTIK. J Exp Bot **65:** 6499–6512

Guzel Deger A, Scherzer S, Nuhkat M, Kedzierska J, Kollist H, Brosché M, Unyayar S, Boudsocq M, Hedrich R, Roelfsema MR (2015) Guard cell SLAC1-type anion channels mediate flagellin-induced stomatal closure. New Phytol **208:** 162–173

Hamilton DW, Hills A, Kohler B, Blatt MR (2000) Ca^{2+} channels at the plasma membrane of stomatal guard cells are activated by hyperpolarization and abscisic acid. Proc Natl Acad Sci USA **97:** 4967–4972

Hao LH, Wang WX, Chen C, Wang YF, Liu T, Li X, Shang ZL (2012) Extracellular ATP promotes stomatal opening of *Arabidopsis thaliana* through heterotrimeric G protein α subunit and reactive oxygen species. Mol Plant **5:** 852–864

Hikagi T, Kutsuna N, Sano T, Kondo N, Hasezawa S (2010) Quantification and cluster analysis of actin cytoskeletal structures in plant cells: Role of actin bundling in stomatal movement during diurnal cycles in Arabidopsis guard cells. Plant J **61:** 156–165

Jevtić P, Edens LJ, Vuković LD, Levy DL (2014) Sizing and shaping the nucleus: Mechanisms and significance. Curr Opin Cell Biol **28:** 16–27

Jezek M, Blatt MR (2017) The membrane transport system of the guard cell and its integration for stomatal dynamics. Plant Physiol **174:** 487–519

Jiang K, Sorefan K, Deeks MJ, Bevan MW, Hussey PJ, Hetherington AM (2012) The ARP2/3 complex mediates guard cell actin reorganization and stomatal movement in Arabidopsis. Plant Cell **24:** 2031–2040

Jiang Y, Wu K, Lin F, Qu Y, Liu X, Zhang Q (2014) Phosphatidic acid integrates calcium signaling and microtubule dynamics into regulating ABA-induced stomatal closure in Arabidopsis. Planta **239:** 565–575

Kanchiswamy C, Malnoy M, Occhipinti A, Maffei M (2014) Calcium imaging perspectives in plants. Int J of Mol Sci **15:** 3842–3859

Kang JY, Choi HI, Im MY, Kim SY (2002) Arabidopsis basic leucine zipper proteins that mediate stress-responsive abscisic acid signaling. Plant Cell **14:** 343–357

Kim M, Hepler PK, Eun SO, Ha KS, Lee Y (1995) Actin filaments in mature guard cells are radially distributed and involved in stomatal movement. Plant Physiol **109:** 1077–1084

Kim TH, Böhmer M, Hu H, Nishimura N, Schroeder JI (2010) Guard cell signal transduction network: Advances in understanding abscisic acid, CO_2, and Ca^{2+} signaling. Annu Rev Plant Biol **61:** 561–591

Kwak JM, Mori IC, Pei ZM, Leonhardt N, Torres MA, Dangl JL, Bloom RE, Bodde S, Jones JD, Schroeder JI (2003) NADPH oxidase AtrbohD and AtrbohF genes function in ROS-dependent ABA signaling in Arabidopsis. EMBO J **22:** 2623–2633

Lemichez E, Wu Y, Sanchez JP, Mettouchi A, Mathur J, Chua NH (2001) Inactivation of AtRac1 by abscisic acid is essential for stomatal closure. Gene Dev **15:** 1808–1816

Lentze N, Auerbach D (2008) Membrane-based yeast two-hybrid system to detect protein interactions. Curr Protoc Protein Sci **19:** 9.17

Leyman B, Geelen D, Quintero FJ, Blatt MR (1999) A tobacco syntaxin with a role in hormonal control of guard cell ion channels. Science **283:** 537–540

Li X, Li JH, Wang W, Chen NZ, Ma TS, Xi YN, Zhang XL, Lin HF, Bai Y, Huang SJ, et al (2014) ARP2/3 complex-mediated actin dynamics is required for hydrogen peroxide-induced stomatal closure in Arabidopsis. Plant Cell Environ **37:** 1548–1560

Lucas JR, Nadeau JA, Sack FD (2006) Microtubule arrays and *Arabidopsis* stomatal development. J Exp Bot **57:** 71–79

Lv XB, Liu L, Cheng C, Yu B, Xiong L, Hu K, Tang J, Zeng L, Sang Y (2015) SUN2 exerts tumor suppressor functions by suppressing the Warburg effect in lung cancer. Sci Rep **5:** 17940

MacRobbie EA, Kurup S (2007) Signalling mechanisms in the regulation of vacuolar ion release in guard cells. New Phytol **175:** 630–640

Merilo E, Laanemets K, Hu H, Xue S, Jakobson L, Tulva I, Gonzalez-Guzman M, Rodriguez PL, Schroeder JI, Broschè M, et al (2013) PYR/RCAR receptors contribute to ozone-, reduced air humidity-, darkness-, and CO_2-induced stomatal regulation. Plant Physiol **162:** 1652–1668

Mustilli AC, Merlot S, Vavasseur A, Fenzi F, Giraudat J (2002) Arabidopsis OST1 protein kinase mediates the regulation of stomatal aperture by abscisic acid and acts upstream of reactive oxygen species production. Plant Cell **14:** 3089–3099

Nadeau JA, Sack FD (2002) Stomatal development in Arabidopsis. The Arabidopsis Book **1:** e0066. doi:10.1199/tab.0162

Oda Y, Fukuda H (2011) Dynamics of Arabidopsis SUN proteins during mitosis and their involvement in nuclear shaping. Plant J **66:** 629–641

Ogasawara Y, Kaya H, Hiraoka G, Yumoto F, Kimura S, Kadota Y, Hishinuma H, Senzaki E, Yamagoe S, Nagata K, et al (2008) Synergistic activation of the Arabidopsis NADPH oxidase AtrbohD by Ca^{2+} and phosphorylation. J Biol Chem **283:** 8885–8892

Pei ZM, Murata Y, Benning G, Thomine S, Klüsener B, Allen GJ, Grill E, Schroeder JI (2000) Calcium channels activated by hydrogen peroxide mediate abscisic acid signalling in guard cells. Nature **406:** 731–734

Poulet A, Probst AV, Graumann K, Tatout C, Evans D (2017) Exploring the evolution of the proteins of the plant nuclear envelope. Nucleus **8:** 46–59

Schroeder JI, Allen GJ, Hugouvieux V, Kwak JM, Waner D (2001a) Guard cell signal transduction. Annu Rev Plant Physiol Plant Mol Biol **52:** 627–658

Schroeder JI, Kwak JM, Allen GJ (2001b) Guard cell abscisic acid signalling and engineering drought hardiness in plants. Nature **410:** 327–330

Sokolovski S, Hills A, Gay RA, Blatt MR (2008) Functional interaction of the SNARE protein NtSyp121 in Ca^{2+} channel gating, Ca^{2+} transients and ABA signalling of stomatal guard cells. Mol Plant **1:** 347–358

Staiger CJ, Sheahan MB, Khurana P, Wang X, McCurdy DW, Blanchoin L (2009) Actin filament dynamics are dominated by rapid growth and severing activity in the Arabidopsis cortical array. J Cell Biol **184:** 269–280

Sutter JU, Campanoni P, Tyrrell M, Blatt MR (2006) Selective mobility and sensitivity to SNAREs is exhibited by the Arabidopsis KAT1 K^+ channel at the plasma membrane. Plant Cell **18:** 935–954

Sutter JU, Sieben C, Hartel A, Eisenach C, Thiel G, Blatt MR (2007) Abscisic acid triggers the endocytosis of the Arabidopsis KAT1 K^+ channel and its recycling to the plasma membrane. Curr Biol **17:** 1396–1402

Tamura K, Goto C, Hara-Nishimura I (2015) Recent advances in understanding plant nuclear envelope proteins involved in nuclear morphology. J Exp Bot **66:** 1641–1647

Tamura K, Iwabuchi K, Fukao Y, Kondo M, Okamoto K, Ueda H, Nishimura M, Hara-Nishimura I (2013) Myosin XI-i links the nuclear membrane to the cytoskeleton to control nuclear movement and shape in Arabidopsis. Curr Biol **23:** 1776–1781

Uddin MN, Akhter S, Chakraborty R, Baek JH, Cha JY, Park SJ, Kang H, Kim WY, Lee SY, Mackey D, et al (2017) SDE5, a putative RNA export protein, participates in plant innate immunity through a flagellin-dependent signaling pathway in Arabidopsis. Sci Rep **7:** 9859

Umezawa T, Nakashima K, Miyakawa T, Kuromori T, Tanokura M, Shinozaki K, Yamaguchi-Shinozaki K (2010) Molecular basis of the core regulatory network in ABA responses: Sensing, signaling and transport. Plant Cell Physiol **51:** 1821–1839

Verma V, Ravindran P, Kumar PP (2016) Plant hormone-mediated regulation of stress responses. BMC Plant Biol **16:** 86

Wang F, Jia J, Wang Y, Wang W, Chen Y, Liu T, Shang Z (2014) Hyperpolarization-activated Ca^{2+} channels in guard cell plasma membrane are involved in extracellular ATP-promoted stomatal opening in *Vicia faba*. J Plant Physiol **171:** 1241–1247

Wang Y, Chen ZH, Zhang B, Hills A, Blatt MR (2013) PYR/PYL/RCAR abscisic acid receptors regulate K+ and Cl- channels through reactive oxygen species-mediated activation of Ca^{2+} channels at the plasma membrane of intact Arabidopsis guard cells. Plant Physiol **163:** 566–577

Xi W, Liu C, Hou X, Yu H (2010) MOTHER OF FT AND TFL1 regulates seed germination through a negative feedback loop modulating ABA signaling in Arabidopsis. Plant Cell **22:** 1733–1748

Xiao Y, Chen Y, Huang R, Chen J, Wang XC (2004) Depolymerization of actin cytoskeleton is involved in stomatal closure-induced by extracellular calmodulin in Arabidopsis. Sci China C Life Sci **47:** 454–460

Yin Y, Adachi Y, Ye W, Hayashi M, Nakamura Y, Kinoshita T, Mori IC, Murata Y (2013) Difference in abscisic acid perception mechanisms between closure induction and opening inhibition of stomata. Plant Physiol **163:** 600–610

Zhang JF, Yuan LJ, Shao Y, Du W, Yan DW, Lu YT (2008a) The disturbance of small RNA pathways enhanced abscisic acid response and multiple stress responses in Arabidopsis. Plant Cell Environ **31:** 562–574

Zhang W, He SY, Assmann SM (2008b) The plant innate immunity response in stomatal guard cells invokes G-protein-dependent ion channel regulation. Plant J **56:** 984–996

Zhao S, Jiang Y, Zhao Y, Huang S, Yuan M, Zhao Y, Guo Y (2016) CASEIN KINASE1-LIKE PROTEIN2 regulates actin filament stability and stomatal closure via phosphorylation of Actin Depolymerizing Factor. Plant Cell **28:** 1422–1439

Zhao Y, Zhao S, Mao T, Qu X, Cao W, Zhang L, Zhang W, He L, Li S, Ren S, et al (2011) The plant-specific actin binding protein SCAB1 stabilizes actin filaments and regulates stomatal movement in Arabidopsis. Plant Cell **23:** 2314–2330

Zhou X, Graumann K, Evans DE, Meier I (2012) Novel plant SUN-KASH bridges are involved in RanGAP anchoring and nuclear shape determination. J Cell Biol **196:** 203–211

Zhou X, Graumann K, Wirthmueller L, Jones JD, Meier I (2014) Identification of unique SUN-interacting nuclear envelope proteins with diverse functions in plants. J Cell Biol **205:** 677–692

Zhou X, Groves NR, Meier I (2015) SUN anchors pollen WIP–WIT complexes at the vegetative nuclear envelope and is necessary for pollen tube targeting and fertility. J Exp Bot **66:** 7299–7307

Zhou X, Meier I (2014) Efficient plant male fertility depends on vegetative nuclear movement mediated by two families of plant outer nuclear membrane proteins. Proc Natl Acad Sci USA **111:** 11900–11905

Zhou X, Meier I (2013) How plants LINC the SUN to KASH. Nucleus **4:** 206–215

Zou JJ, Li XD, Ratnasekera D, Wang C, Liu WX, Song LF, Zhang WZ, Wu WH (2015) Arabidopsis CALCIUM-DEPENDENT PROTEIN KINASE8 and CATALASE3 function in abscisic acid-mediated signaling and H_2O_2 homeostasis in stomatal guard cells under drought stress. Plant Cell **27:** 1445–1460